Brief paper

Design and implementation of an autonomous flight control law for a UAV helicopter☆

Kemao Peng [a], Guowei Cai [b], Ben M. Chen [b,*], Miaobo Dong [b], Kai Yew Lum [a,b], Tong H. Lee [b]

[a] Temasek Laboratories, National University of Singapore, Singapore 117508, Singapore
[b] Department of Electrical and Computer Engineering, National University of Singapore, Singapore 117576, Singapore

A B S T R A C T

In this paper, we present the design and implementation of an autonomous flight control law for a small-scale unmanned aerial vehicle (UAV) helicopter. The approach is decentralized in nature by incorporating a newly developed nonlinear control technique, namely the composite nonlinear feedback control, together with dynamic inversion. The overall control law consists of three hierarchical layers, namely, the kernel control, command generator and flight scheduling, and is implemented and verified in flight tests on the actual UAV helicopter. The flight test results demonstrate that the UAV helicopter is capable of carrying out complicated flight missions autonomously.

© 2009 Elsevier Ltd. All rights reserved.

1. Introduction

Unmanned aerial vehicles (UAVs) have recently aroused great interest in industrial and academic circles, because of their potential applications in many areas and their scientific significance in academic research. UAVs are capable of carrying out work where the surrounding environment is dangerous to human beings and they can be utilized as platforms with maneuverability and versatility for pure academic research. Among various types of UAVs, the UAV helicopter is an excellent platform for academic research as it is safely manipulated in a manual mode and is easily operated in an automatic mode. Many research groups worldwide have chosen such a platform for their academic purposes (see, for examples, Bortoff (1999), Kim, Shim, and Sastry (2002), McKerrow (2004), Roberts, Corke, and Buskey (2002) and Shim, Kim, and Sastry (2000), and the references therein).

Small-scale UAV helicopters are commonly upgraded from radio-controlled hobby helicopters by assembling an avionics system (Cai, Peng, Chen, & Lee, 2005; Sprague et al., 2001). The function of the avionics system is to collect measurement signals, drive the actuators, and support communications and real-time operations of autonomous flight control laws. One of the core issues in designing a fully autonomous UAV helicopter is to effectively design and implement sophisticated flight control laws. Diverse methods, such as H_∞ control (Weilenmann, Christen, & Geering, 1999), the model predictive approach (Shim, Kim, & Sastry, 2003), the differential geometry method (Isidori, Marconi, & Serrani, 2003) and the neural network approach (Enns & Si, 2003), have been explored to design autonomous flight control laws for small-scale UAV helicopters. The work of (Marconi & Naldi, 2007) provides some useful theoretical guidelines in controlling helicopters. However, many of the works focus merely on the design of kernel control laws and/or in certain specific flight conditions and are only verified by simulation.

The objective of our work is to design a fully autonomous flight control law that is able to perform various flight missions for a UAV helicopter, and to verify the feasibility and operability of the UAV in actual flight tests. The proposed flight control scheme consists of three parts, namely, the kernel control law, command generator and flight scheduling. The function of the kernel control law is to guarantee the asymptotic stability of the aircraft motion with respect to the surrounding air. The role of the command generator is to produce flight commands or references to the kernel control layer, and finally the task of the flight scheduling part is to generate the flight references for pre-scheduled flight tasks or flight missions. Since the time scale associated each part of the overall flight control system is hierarchical in nature, the

* Corresponding author. Tel.: +65 6516 2289; fax: +65 6779 1103.
E-mail addresses: kmpeng@nus.edu.sg (K. Peng), caiguowei@nus.edu.sg (G. Cai), bmchen@nus.edu.sg, bmchen@ieee.org (B.M. Chen), eledm@nus.edu.sg (M. Dong), kaiyew_lum@nus.edu.sg (K.Y. Lum), eleleeth@nus.edu.sg (T.H. Lee).

flight control law can be designed in a decentralized fashion. A newly developed nonlinear control technique, namely, the composite nonlinear feedback (CNF) control method (Chen, Lee, Peng, & Venkataramanan, 2003; He, Chen, & Wu, 2005), which has successfully been applied to solve many real-life problems, is employed to design the kernel control law based on the identified linear model of the UAV helicopter using in-flight data. Dynamic inversion (Isidori et al., 2003), capable of fully dealing with nonlinearities in affine systems, is adopted to design the command generator based on the kinematical models of the UAV. Lastly, the flight scheduling is described in a discrete event system that causes the helicopter to fly in some pre-determined flight conditions.

2. Dynamic and kinematic models of UAV helicopter

The UAV system studied in this paper, named HeLion, is upgraded from a radio-controlled bare helicopter, Raptor 90, by assembling an effective avionics onboard system mounted under the fuselage of the helicopter (Cai et al., 2005). The helicopter is 1,410 mm in length, 190 mm in width, and 476 mm in height, and its maximal takeoff weight is 15 kg. Its weight increases from 4.9 kg to 11 kg after integrating all the necessary components. Its main rotor has a diameter of 1,605 mm and its tail rotor has a diameter of 260 mm. The helicopter is equipped with an engine, which produces a power of 2.28 kW at the spinning rate of 15,000 rpm, and it can be operated manually with a remote control unit. The range of its practical spinning rate is from 2,000 rpm to 16,000 rpm. The gear ratio of the engine rotor to the main rotor to the tail rotor is 8.45:1:4.65. The bare helicopter is capable of performing various flight tasks including hover and agile flight. As the flight speed of small-scale helicopters is relatively low, its effect in aerodynamics can be safely ignored and it is feasible practically to use a linear model in hovering and near-hovering flight conditions. A linear model of HeLion for such flight conditions has been identified in Cai, Chen, Peng, Dong, and Lee (2006) with in-flight data and is given as

$$\begin{pmatrix} \dot{x}_1 \\ \dot{x}_2 \end{pmatrix} = \begin{bmatrix} A_1 & 0 \\ 0 & A_2 \end{bmatrix} \begin{pmatrix} x_1 \\ x_2 \end{pmatrix} + \begin{bmatrix} B_1 & 0 \\ 0 & B_2 \end{bmatrix} u, \tag{1}$$

where the state variables

$$x_1 = \left(V_x, V_y, \phi, \theta, \omega_x, \omega_y, a, b\right)', \qquad x_2 = \left(V_z, \psi, \omega_z, w_f\right)',$$

and where V_x, V_y, V_z (in m/s) are the ground velocities measured in the (x, y, z)-directions of the body frame, respectively. ϕ, θ and ψ (in rad) are respectively the roll, pitch and yaw angles, and ω_x, ω_y and ω_z (in rad/s) are the corresponding roll, pitch and yaw angular rates, a and b (in rad) are the first harmonics of longitudinal and lateral flapping angles of the main blade tip-path plane, and finally, ω_f is a state variable of a built-in filter in the yaw channel. The control input is given by

$$u = \delta - \delta_0, \tag{2}$$

where δ_0 is the trim values of the control input command, and $\delta = \left(\delta_r, \delta_p, \delta_c, \delta_t\right)'$, with δ_r, δ_p, δ_c and δ_t being respectively the roll cyclic, pitch cyclic, collective and tail rotor commands, which all have a normalized value in $[-1, 1]$, with 1 being equivalent to $\pi/4$ rad. For HeLion, the maximum values that the input channels can take are respectively 0.35, 0.35, 0.12 and 0.4. The measurement output of the UAV system is

$$y = \left(V_x, V_y, \phi, \theta, \omega_x, \omega_y, V_z, \psi, \omega_z\right)'. \tag{3}$$

In the hovering condition, $\delta_0 = (0.05, 0.02, -0.22, 0)'$ when the spinning rate of the main blades is 1750 rpm. Under such an operating condition, the corresponding system data are

$$A_1 = \begin{bmatrix} A_{11} & A_{12} & 0 & A_{14} \\ 0 & 0 & I_2 & 0 \\ A_{31} & 0 & 0 & A_{34} \\ 0 & 0 & A_{43} & A_{44} \end{bmatrix}, \qquad B_1 = \begin{bmatrix} 0 \\ 0 \\ 0 \\ B_{41} \end{bmatrix},$$

$$A_2 = \begin{bmatrix} A_{55} & A_{56} & 0 \\ 0 & A_{66} & 0 \\ A_{75} & A_{76} & A_{77} \\ 0 & A_{86} & A_{87} \end{bmatrix}, \qquad B_2 = \begin{bmatrix} B_{52} & 0 \\ 0 & 0 \\ B_{72} & B_{73} \\ 0 & 0 \end{bmatrix},$$

where

$$A_{11} = \begin{bmatrix} -0.1778 & 0 \\ 0 & -0.3104 \end{bmatrix}, \qquad A_{12} = \begin{bmatrix} 0 & -9.781 \\ 9.781 & 0 \end{bmatrix},$$

$$A_{14} = \begin{bmatrix} -9.781 & 0 \\ 0 & 9.781 \end{bmatrix}, \qquad A_{31} = \begin{bmatrix} -0.3326 & -0.5353 \\ 0.1903 & -0.2940 \end{bmatrix},$$

$$A_{34} = \begin{bmatrix} 75.764 & 343.860 \\ 172.620 & -59.958 \end{bmatrix}, \qquad A_{43} = \begin{bmatrix} 0 & -1 \\ -1 & 0 \end{bmatrix},$$

$$A_{44} = \begin{bmatrix} -8.1222 & 4.6535 \\ -0.0921 & -8.1222 \end{bmatrix}, \qquad A_{55} = -0.6821,$$

$$A_{56} = \begin{bmatrix} 0 & -0.1070 \end{bmatrix}, \qquad A_{66} = \begin{bmatrix} 0 & 1 \end{bmatrix},$$

$$A_{76} = \begin{bmatrix} 0 & -5.5561 \end{bmatrix}, \qquad A_{86} = \begin{bmatrix} 0 & 2.7492 \end{bmatrix},$$

$$A_{75} = -0.1446, \qquad A_{77} = -36.674, \qquad A_{87} = -11.1120,$$

$$B_{41} = \begin{bmatrix} 0.0496 & 2.6224 \\ 2.4928 & 0.1740 \end{bmatrix}, \qquad B_{52} = 15.6491,$$

$$B_{72} = 1.6349, \qquad B_{73} = -58.4053.$$

The kinematical model is relatively simple and is given by

$$\begin{pmatrix} \dot{p}_x \\ \dot{p}_y \\ \dot{p}_z \end{pmatrix} = B'_b \begin{pmatrix} V_x \\ V_y \\ V_z \end{pmatrix}, \tag{4}$$

where p_x, p_y, p_z are respectively the displacements (in m) of helicopter in the (x, y, z)-directions of the north-east-down (NED) frame, and B_b is the transformation matrix from the NED frame to the body frame with

$$B_b = \begin{bmatrix} c_\theta c_\psi & c_\theta s_\psi & -s_\theta \\ -c_\phi s_\psi + s_\phi s_\theta c_\psi & c_\phi c_\psi + s_\phi s_\theta s_\psi & s_\phi c_\theta \\ s_\phi s_\psi + c_\phi s_\theta c_\psi & -s_\phi c_\psi + c_\phi s_\theta s_\psi & c_\phi c_\theta \end{bmatrix}, \tag{5}$$

where $s_\star = \sin(\star)$ and $c_\star = \cos(\star)$. Lastly, the height of the aircraft is given by $h = -p_z$.

3. Design of autonomous flight control law

The schematic diagram of the autonomous flight control law is shown in Fig. 1, in which the overall flight control system is hierarchically divided into three layers: (1) the kernel control layer, which is to guarantee the asymptotic stability of the aircraft motion with respect to the surrounding air and to track flight commands V_{xc}, V_{yc}, V_{zc}, and ψ_c; (2) the command generator layer, which is to generate flight commands by tracking flight references p_{xr}, p_{yr} and p_{zr} from the flight scheduling layer; and lastly (3) the flight scheduling layer, which is to generate flight references based on pre-schedule flight tasks or flight missions. As demonstrated later in actual test results, such a control scheme has proven to be very effective and yields an excellent performance.

3.1. Kernel control layer

The structure of the kernel control law is decentralized in nature and is shown in Fig. 2. The kernel control law is decoupled into two parts, i.e., the rolling/pitching control and the heaving/heading control. The rolling/pitching control is hierarchically divided into the velocity, attitude and swashplate control components. The
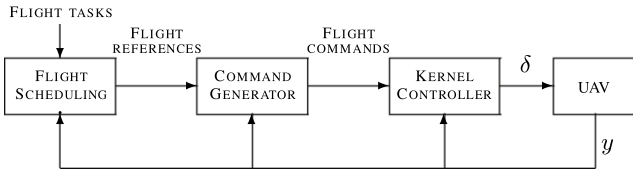
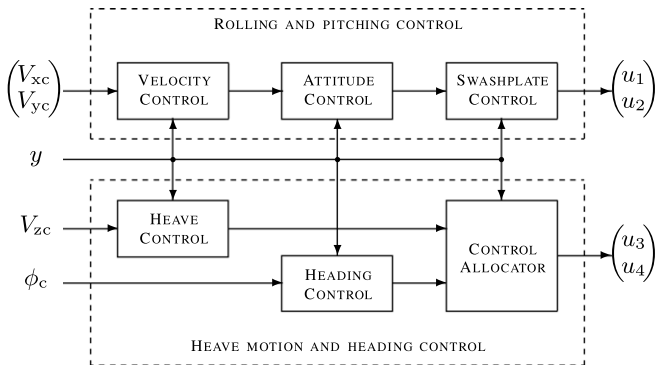**Fig. 1.** Structure of the overall autonomous flight control.

Fig. 2. Structure of the kernel control system.

heaving/heading control is respectively decoupled into the heaving and heading components. The velocity, swashplate and heaving control components are designed with the pole assignment method, whereas the attitude and heading control laws are designed using the CNF control technique. The CNF controller consists of a linear feedback control law and a nonlinear feedback control law. The linear feedback law is designed to yield a closed-loop system with a small damping ratio for a quick response, while the nonlinear feedback law is used to increase the damping ratio of the closed-loop system, when the system output approaches the target reference, to reduce the overshoot. We refer interested readers to Chen et al. (2003) and He et al. (2005) for more detailed information on the CNF control technique. Information on hardware components used in actual flight implementation can be found in Cai et al. (2005).

3.1.1. Velocity control

The role of the velocity control is to design a control law such that the state variables of V_x and V_y are capable of tracking the flight commands V_{xc} and V_{yc} as quickly as possible. The velocity control law is carried out based on the following subsystem

$$\dot{x}_{11} = \bar{A}_{11}x_{11} + A_{12}v_{11}, \tag{6}$$

where $x_{11} = (V_x, V_y)'$, $\bar{A}_{11} = A_{11} - A_{14}A_{34}^{-1}A_{31}$ and

$$v_{11} = x_{31} + A_{12}^{-1}A_{14}\left[x_{44} + A_{34}^{-1}A_{31}x_{11}\right], \tag{7}$$

where $x_{31} = (\phi, \theta)'$ and $x_{44} = (a, b)'$. We note that the term associated with x_{11} is introduced in v_{11} to deal with the interaction between the velocity and attitude control. An appropriate control law is then obtained and is given by

$$v_{11} = F_{11}x_{11} + G_{11}\begin{pmatrix} V_{xc} \\ V_{yc} \end{pmatrix}, \tag{8}$$

where

$$F_{11} = \begin{bmatrix} -0.00579 & -0.11821 \\ 0.11702 & -0.00116 \end{bmatrix} \tag{9}$$

is chosen such that $\bar{A}_{11} + A_{12}F_{11}$ is asymptotically stable, and $G_{11} = -A_{12}^{-1}(\bar{A}_{11} + A_{12}F_{11})$.

3.1.2. Attitude control

The attitude controller is designed based on the following subsystem

$$\dot{x}_{33} = A_\Phi x_{33} + B_\Phi v_{33}, \qquad z_{33} = C_{\Phi 2}x_{33} + D_{\Phi 2}v_{33}, \tag{10}$$

where $x_{33} = (\phi, \theta, \omega_x, \omega_y)'$,

$$A_\Phi = \begin{bmatrix} 0 & I_2 \\ 0 & 0 \end{bmatrix}, \qquad B_\Phi = \begin{bmatrix} 0 \\ A_{34} \end{bmatrix}, \tag{11}$$

the control input

$$v_{33} = x_{44} + A_{34}^{-1}A_{31}x_{11}, \tag{12}$$

and the controlled output z_{33} is characterized by

$$C_{\Phi 2} = \begin{bmatrix} I_2 & 0 \end{bmatrix}, \qquad D_{\Phi 2} = A_{12}^{-1}A_{14}. \tag{13}$$

Attitude control is to make z_{33} track the signal v_{11} of (8). Following the design procedure of (Chen et al., 2003; He et al., 2005), a state feedback CNF control law is obtained and is given by

$$v_{33} = F_\Phi x_{33} + G_\Phi v_{11} + \rho_\Phi B_\Phi' P_\Phi \left[x_{33} - H_\Phi v_{11}\right], \tag{14}$$

where

$$F_\Phi = \begin{bmatrix} -0.04802 & -0.17774 & -0.02595 & -0.09596 \\ -0.10928 & 0.01683 & -0.06395 & 0.01119 \end{bmatrix}$$

is selected such that $A_\Phi + B_\Phi F_\Phi$ is asymptotically stable,

$$G_\Phi = [D_{\Phi 2} - (C_{\Phi 2} + D_{\Phi 2}F_\Phi)(A_\Phi + B_\Phi F_\Phi)^{-1}B_\Phi]^{-1},$$

$$H_\Phi = -(A_\Phi + B_\Phi F_\Phi)^{-1}B_\Phi G_\Phi, \tag{15}$$

and $P_\Phi > 0$ is the solution of the Lyapunov equation,

$$(A_\Phi + B_\Phi F_\Phi)'P_\Phi + P_\Phi(A_\Phi + B_\Phi F_\Phi) = -W_\Phi \tag{16}$$

with $W_\phi = \text{diag}\{0.01, 0, 01, 0.001, 0.001\}$,

$$\rho_\Phi = \text{diag}\left\{-\beta_1\left|\frac{e^{-\alpha_1|\tilde{\phi}|} - e^{-1}}{1 - e^{-1}}\right|, -\beta_2\left|\frac{e^{-\alpha_2|\tilde{\theta}|} - e^{-1}}{1 - e^{-1}}\right|\right\}$$

with $\beta_1 = 1$, $\alpha_1 = 0.1$ and $\beta_2 = 0.6$, $\alpha_2 = 0.1$, and

$$\begin{pmatrix} \tilde{\phi} \\ \tilde{\theta} \end{pmatrix} = x_{31} - \left[I_2 - A_{12}^{-1}A_{14}(F_\Phi H_\Phi + G_\Phi)\right]v_{11}. \tag{17}$$

3.1.3. Swashplate control

To design a swashplate controller, we consider the following subsystem characterized by

$$\dot{x}_{44} = A_{44}x_{44} + B_{41}v_{44}, \tag{18}$$

where $x_{44} = (a, b)'$, and the control input

$$v_{44} = B_{41}^{-1}A_{43}x_{32} + \begin{pmatrix} u_1 \\ u_2 \end{pmatrix}, \tag{19}$$

and where $x_{32} = (\omega_x, \omega_y)'$, and u_1 and u_2 are respectively the first and second entries of the UAV model in (1). It is to design a control law that such that x_{44} tracks

$$r_{44} = v_{33} - A_{34}^{-1}A_{31}x_{11}. \tag{20}$$

For this subsystem, the state variables cannot be measured. We would thus have to design a dynamic output feedback control law instead. The following is an appropriate controller for controlling the swashplate of the helicopter,

$$\dot{x}_{c44} = (A_{44} - L_{44}A_{34})x_{c44} - L_{44}A_{31}x_{11} + B_{41}v_{44} + (A_{44} - L_{44}A_{34})L_{44}x_{32} \tag{21}$$

and

$$v_{44} = F_{44}(x_{c44} + L_{44}x_{32}) + G_{44}r_{44}, \tag{22}$$

where

$$L_{44} = \begin{bmatrix} 0.010 & 0.025 \\ 0.025 & 0.010 \end{bmatrix}, \qquad F_{44} = \begin{bmatrix} -0.2605 & -3.4751 \\ -1.2188 & -0.4924 \end{bmatrix}$$

are chosen such that $A_{44} - L_{44}A_{34}$ and $A_{44} + B_{41}F_{44}$ are stable, and $G_{44} = -B_{41}^{-1}(A_{44} + B_{41}F_{44})$. Finally,

$$\begin{pmatrix} u_1 \\ u_2 \end{pmatrix} = v_{44} - B_{41}^{-1}A_{43}x_{32}. \tag{23}$$

3.1.4. Heave motion control

This part is to control V_z tracking the flight command V_{zc}. To control the heave direction motion of the UAV helicopter, we use the following subsystem

$$\dot{V}_z = A_{55}V_z + B_{52}v_{55}, \tag{24}$$

where the control input variable

$$v_{55} = B_{52}^{-1}A_{56}x_{66} + u_3, \tag{25}$$

and where $x_{66} = (\psi, \omega_z)'$ and u_3 is the third entry in the control input vector of (1). A very simple static controller is obtained as follows

$$v_{55} = F_{55}V_z - B_{52}^{-1}(A_{55} + B_{52}F_{55})V_{zc}. \tag{26}$$

We select $F_{55} = -0.052265$ such that $A_{55} + B_{52}F_{55} < 0$. It is clear that

$$u_3 = v_{55} - B_{52}^{-1}A_{56}x_{66}. \tag{27}$$

3.1.5. Heading motion control

Heading motion control is to generate a controller such that the state variable ψ will follow the flight command ψ_c. The subsystem we use for heading motion control is characterized by

$$\dot{x}_{66} = A_\psi x_{66} + B_\psi v_{66}, \tag{28}$$

where $x_{66} = (\psi, \omega_z)'$,

$$A_\psi = \begin{bmatrix} A_{66} \\ A_{76} \end{bmatrix}, \qquad B_\psi = \begin{bmatrix} 0 \\ B_{73} \end{bmatrix}. \tag{29}$$

The following state feedback CNF control law yields a very good performance for the heading motion:

$$v_{66} = F_\psi x_{66} + G_\psi \psi_c + \rho_\psi B_\psi' P_\psi (x_{66} - H_\psi \psi_c), \tag{30}$$

where

$$F_\psi = \begin{bmatrix} 0.01712 & -0.08486 \end{bmatrix} \tag{31}$$

is chosen such that $A_\psi + B_\psi F_\psi$ is asymptotically stable,

$$G_\psi = [-C_{\psi 2}(A_\psi + B_\psi F_\psi)^{-1}B_\psi]^{-1}, \tag{32}$$

$$H_\psi = -(A_\psi + B_\psi F_\psi)^{-1}B_\psi G_\psi, \tag{33}$$

$P_\psi > 0$ is the solution of the Lyapunov equation,

$$(A_\psi + B_\psi F_\psi)'P_\psi + P_\psi(A_\psi + B_\psi F_\psi) = -W_\psi \tag{34}$$

with $W_\psi = \text{diag}\{0.034243, 1.7122 \times 10^{-6}\}$, and finally

$$\rho_\psi = -\beta_4 \left| \frac{e^{-\alpha_4|\psi - \psi_c|} - e^{-1}}{1 - e^{-1}} \right| \tag{35}$$

with $\beta_4 = 1$ and $\alpha_4 = 0.1$.

In order to transform the control law of (30) into the actual input to the helicopter, we need to estimate the state variable ω_f associated to the built-in filter in the yaw channel, which can be done as follows

$$\dot{x}_f = (A_{87} - L_f A_{77})(x_f + L_f \omega_z) + A_{86}x_{66}$$
$$- L_f (A_{75}V_z + A_{76}x_{66} + B_{72}u_3 + B_{73}u_4), \tag{36}$$

where $L_f = -0.1$ is chosen so that $A_{87} - L_f A_{77} < 0$, and

$$\hat{\omega}_f = x_f + L_f \omega_z. \tag{37}$$

Finally, the 4th entry of the control input vector is given by

$$u_4 = v_{66} - B_{73}^{-1}(A_{75}V_z - A_{77}\hat{\omega}_f - B_{72}u_3) \tag{38}$$

and the actual control signal that is injected into the UAV is given by

$$\delta = \delta_0 + u. \tag{39}$$

This completes the design of the kernel control laws for the UAV helicopter system.

3.2. Command generator

The command generator function is to generate necessary flight commands associated with required flight missions. It can be carried out using the dynamic inversion technique based on the displacement equation or the kinematic model of the UAV system in (4). More specifically, we note that (4) can be rewritten as

$$\begin{pmatrix} \dot{p}_x \\ \dot{p}_y \\ \dot{p}_z \end{pmatrix} = B_b' \begin{pmatrix} V_x \\ V_y \\ V_z \end{pmatrix} = V_g \begin{pmatrix} \cos\psi_s \cos\theta_s \\ \sin\psi_s \cos\theta_s \\ -\sin\theta_s \end{pmatrix}, \tag{40}$$

where V_g, θ_s and ψ_s are respectively the ground speed, flight path angle and flight azimuth angle. The task of the command generator is to generate flight commands, i.e., V_{xc}, V_{yc}, V_{zc} and ψ_c, by tracking the flight references of the scheduled steady and maneuvering flights.

For a heading direction reference given in terms of ψ_r or $\dot{\psi}_r$,

$$\psi_c = \psi_r \quad \text{or} \quad \psi_c = \dot{\psi}_r \Delta t + \psi, \tag{41}$$

where Δt is generally chosen to be the sampling period of the overall control system, which is 20 ms for HeLion. For flight references given in terms of p_{xr}, p_{yr} and p_{zr} or $\dot{h}_r$,

$$\begin{pmatrix} V_{xc} \\ V_{yc} \\ V_{zc} \end{pmatrix} = B_b \begin{bmatrix} k_{px}(p_x - p_{xr}) \\ k_{py}(p_y - p_{yr}) \\ k_{pz}(p_z - p_{zr}) \end{bmatrix} \tag{42}$$

where the last entry $k_{pz}(p_z - p_{zr})$ can be replaced by $-\dot{h}_r$ if it is given, and

$$k_{px} = -0.3, \qquad k_{py} = -0.3, \qquad k_{pz} = -0.5 \tag{43}$$

are feedback gains chosen for our UAV helicopter. We note that $h = -p_z$. For flight references given in terms of V_{gr} and either one of h_r, θ_{sr}, $\dot{\theta}_{sr}$ and ψ_{sr} or $\dot{\psi}_{sr}$,

$$\begin{pmatrix} V_{xc} \\ V_{yc} \\ V_{zc} \end{pmatrix} = B_b V_{gr} \begin{pmatrix} \cos\psi_{sc} \cos\theta_{sc} \\ \sin\psi_{sc} \cos\theta_{sc} \\ -\sin\theta_{sc} \end{pmatrix}, \tag{44}$$

where

$$\theta_{sc} = \arcsin\left\{ \frac{k_h(h - h_r)}{V_g} \right\} \quad \text{or} \quad \theta_{sc} = \dot{\theta}_{sr}\Delta t + \theta_s \tag{45}$$

or $\theta_{sc} = \theta_{sr}$, and

$$\psi_{sc} = \psi_{sr} \quad \text{or} \quad \psi_{sc} = \dot{\psi}_{sr}\Delta t + \psi_s, \tag{46}$$

and where $k_h = -0.5$ is a feedback gain chosen for our UAV and Δt is chosen to be the sampling period of the overall control system.

Lastly, the detailed design of flight scheduling is to be given in the next section for a flight envelope, which consists of flight tasks including automatic takeoff, hovering, slithering, spiraling and automatic landing.

4. Simulation and actual flight experiment

We illustrate the design of flight scheduling with a flight envelope experiment, which consists of tasks including automatic takeoff, hovering, slithering, turning back, head turning, pirouetting, vertical turning, spiral turning, and automatic landing. Table 1 gives the event-driven models of such an experiment. The specific flight references of the scheduled steady and maneuvering flights are given as follows:

(1) Takeoff: $\dot{h}_r$, p_{xr}, p_{yr} and ψ_r are constants.
(2) Hovering: p_{xr}, p_{yr}, p_{zr} and ψ_r are constants.
(3) Slithering: $\psi_{sr} = \psi_{sr0} \pm \pi/4$, and h_r, V_{gr} and ψ_r are constants.
(4) Head turning: h_r, V_{gr}, ψ_{sr} and $\dot{\psi}_r$ are constants.

Table 1
Events in flight scheduling.

| Step No	Flight mission	Transition condition	Next step
0	Abnormal		2
1	Takeoff	Lift up 15 m	2/0
2	Hovering	Duration of 15 s	3/9/A
3	Slithering	Duration of 32 s	4/0
4	Turning back	Duration of 8 s	5/0
5	Head turning	Duration of 32 s	6/0
6	Pirouetting	Duration of 32 s	7/0
7	Vertical turning	Duration of 62.8 s	8/0
8	Spiral turning	Duration of 40 s	2/0
9	Landing	Descend to ground	A/0
A	Termination		
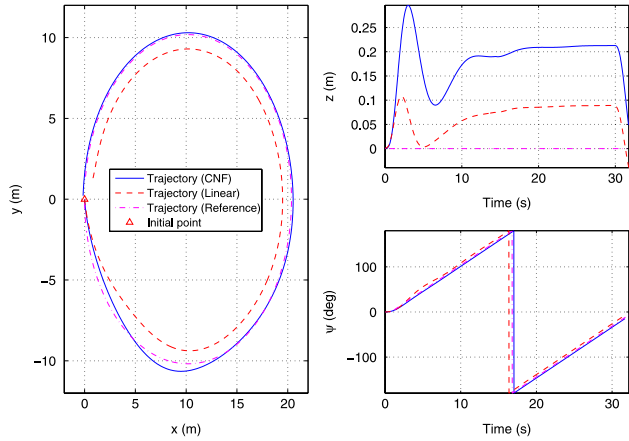
Fig. 3. Position and heading responses of the pirouetting motion.
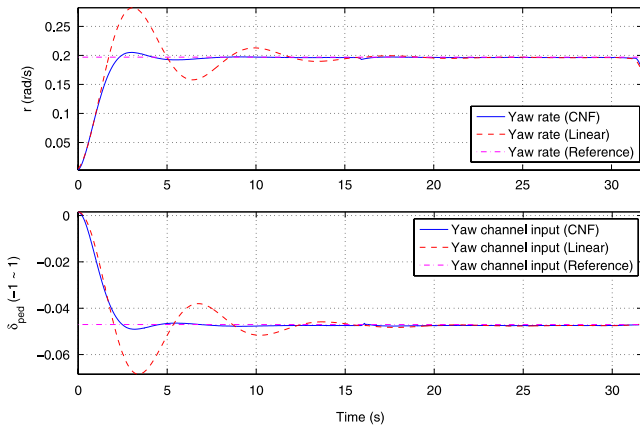

Fig. 4. Yaw rate responses for the pirouetting motion.

(5) Pirouetting: $\psi_r = \psi_s \pm \pi/2$, and h_r, V_{gr} and $\dot{\psi}_{sr}$ are constants.
(6) Vertical turning: V_{gr}, $\dot{\theta}_{sr}$, ψ_{sr} and ψ_r are constants.
(7) Spiral turning: $\psi_r = \psi_s$ or $\psi_r = \psi_s + \pi$, and V_{gr}, θ_{sr} and $\dot{\psi}_{sr}$ are constants.
(8) Landing: $\dot{h}_r$, p_{xr}, p_{yr} and ψ_r are constants.

Before conducting an actual flight for the UAV, we have run a thorough simulation test on the system using our own built hardware-in-the-loop simulation system, in which most of the hardware components of the UAV system, including sensors, servo controllers and wireless communications systems are to be kept in the simulation loop. Shown in Figs. 3 and 4 are the comparison of the performance of the flight control laws designed using the CNF control technique and that of their linear counterparts for the pirouetting motion. It is clear that the nonlinear control laws outperform the linear ones.
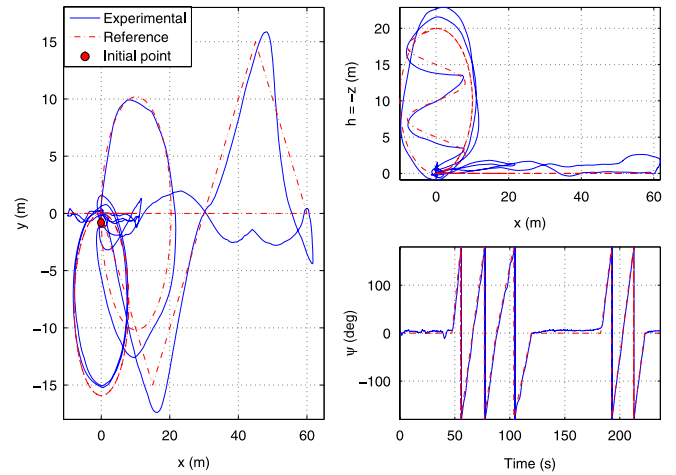

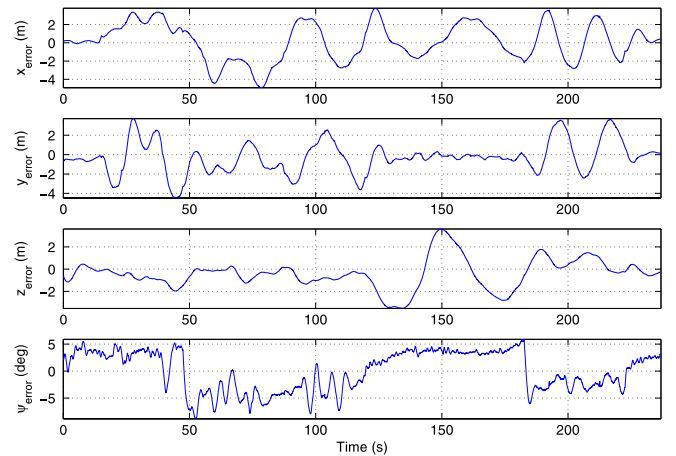**Fig. 5.** Actual flight paths and the references for the whole test.

Fig. 6. Tracking errors for the whole test.

We have conducted actual flight tests of the overall autonomous flight control law on our UAV helicopter, HeLion, together the onboard and ground supporting systems reported in Dong, Chen, Cai, and Peng (2007). The sampling period used in the actual experiment is 20 ms. To have a better sense on the quality of the actual flight test, we show in Fig. 5 the actual position and heading angles of the UAV and their references, and in Fig. 6 the tracking errors throughout the whole test. The results demonstrate that HeLion with the autonomous flight control law effectively completes the scheduled steady and maneuvering flights, and the tracking errors are kept within the GPS accuracy level. Our design is very successful. A video clip captured during the actual test flight can be downloaded or viewed at the following web link, http://uav.ece.nus.edu.sg/~bmchen/reports/fullflight.wmv.

5. Concluding remarks

A fully autonomous flight control law has been designed for our UAV helicopter, HeLion, with a decentralized scheme incorporating the newly developed composite nonlinear control technique and the dynamic inversion approach. The design has also been successfully verified in the actual flight tests. The analysis of the resulting closed-loop system shows that our design has achieved top level flight performance by military standards. Unfortunately, due to space limitation, we are unable to include such a result in the paper. Interested readers can access a full version of this manuscript at http://uav.ece.nus.edu.sg/~bmchen/reports/HeLion.pdf.

References

Bortoff, S. A. (1999). The University of Toronto rc helicopter: A test bed for nonlinear control. In *Proceedings of the 1999 IEEE international conference on control applications* (pp. 333–338).

Cai, G., Chen, B. M., Peng, K., Dong, M., & Lee, T. H. (2006). Modeling and control system design for a UAV helicopter. In *Proceedings of the 14th mediterranean conference on control and automation* (pp. 210–215).

Cai, G., Peng, K., Chen, B. M., & Lee, T. H. (2005). Design and assembling of a uav helicopter system. In *Proceedings of the fifth international conference on control and automation* (pp. 697–702).

Chen, B. M., Lee, T. H., Peng, K., & Venkataramanan, V. (2003). Composite nonlinear feedback control for linear systems with input saturation: Theory and an application. *IEEE Transactions on Automatic Control*, 48, 427–439.

Dong, M., Chen, B. M., Cai, G., & Peng, K. (2007). Development of a real-time onboard and ground station software system for a uav helicopter. *Journal of Aerospace Computing, Information and Communication*, 4, 933–955.

Enns, R., & Si, J. (2003). Helicopter trimming and tracking control using direct neural dynamic programming. *IEEE Transactions on Neural Networks*, 14, 929–939.

He, Y., Chen, B. M., & Wu, C. (2005). Composite nonlinear control with state and measurement feedback for general multivariable systems with input saturation. *Systems and Control Letters*, 54, 455–469.

Isidori, A., Marconi, L., & Serrani, A. (2003). Robust nonlinear motion control of a helicopter. *IEEE Transactions on Automatic Control*, 48, 413–426.

Kim, H. J., Shim, D. H., & Sastry, S. (2002). Flying robots: Modeling, control and decision making. In *Proceedings of the 2002 IEEE international conference on robotics and automation* (pp. 66–71).

Marconi, L., & Naldi, R. (2007). Robust full degree-of-freedom tracking control of a helicopter. *Automatica*, 43, 1909–1920.

McKerrow, P. (2004). Modeling the draganflyer four-rotor helicopter. In *Proceedings of the 2004 IEEE international conference on robotics and automation* (pp. 3596–3601).

Roberts, J. M., Corke, P., & Buskey, G. (2002). Low-cost flight control system for a small autonomous helicopter. In *Proceedings of the 2002 australasian conference on robotics and automation* (pp. 546–551).

Shim, D. H., Kim, H. J., & Sastry, S. (2000). Control system design for rotorcraft-based unmanned aerial vehicle using time-domain system identification. In *Proceedings of the 2000 IEEE international conference on control applications* (pp. 808–813).

Shim, D. H., Kim, H. J., & Sastry, S. (2003). Decentralized nonlinear model predictive control of multiple flying robots. In Proceedings of the 42nd IEEE conference on decision and control (pp. 3621–3626).

Sprague, K., Gavrilets, V., Dugail, D., Mettler, B., Feron, E., & Martinos, I. (2001). Design and applications of an avionics system for a miniature acrobatic helicopter. In *Proceedings of the 20th digital avionics systems conferences*, (p. 3C5/13C5/10).

Weilenmann, M. F., Christen, U., & Geering, H. P. (1999). Robust helicopter position control at hover. In *Proceedings of the 1994 american control conference* (pp. 2491–2495).

Kemao Peng was born in Anhui Province, China, in 1964. He received the B.Eng degree in aircraft control systems, the M.Eng degree in guidance, control, and simulation, and the Ph.D. degree in navigation, guidance and control, all from Beijing University of Aeronautics and Astronautics, Beijing, China, in 1986, 1989, and 1999, respectively.

From 1998 to 2000, he was a postdoctoral research fellow in the School of Automation and Electrical Engineering, Beijing University of Aeronautics and Astronautics. From 2000 to 2006, he was a research fellow in the Department of Electrical and Computer Engineering, National University of Singapore. Since 2006, he has been a research scientist in Temasek Laboratories, National University of Singapore. His current research interests are in nonlinear system control methods, robust control and flight control design.

Dr. Peng is a co-author of a monograph, *Hard Disk Driver Servo Systems*, 2nd Edition (Springer: New York, 2006). He was a recipient of the Best Industrial Control Application Prize at the 5th Asian Control Conference, Melbourne, Australia (2004).

Guowei Cai was born in Tianjin, China, in 1980. He received the B.E. degree in electrical and electronics engineering from Tianjin University, Tianjin, China, in 2002, and the Ph.D. degree in electrical and computer engineering from National University of Singapore, Singapore, in 2009.

Since 2008, he has been a Research Fellow with the Department of Electrical and Computer Engineering, National University of Singapore, Singapore. His current research interests include construction, modeling identification, control theory application, and formation control of small-scale UAV helicopter systems.

Ben M. Chen born in Fuqing, Fujian, China, in 1963, received his B.S. degree in computer science and mathematics from Xiamen University, China, in 1983, an M.S. degree in electrical engineering from Gonzaga University, Spokane, in 1988, and a Ph.D. degree in electrical and computer engineering from Washington State University, Pullman, in 1991.

He was a software engineer in the South-China Computer Corporation, Guangzhou, China, from 1983 to 1986. From 1992 to 1993, he was an Assistant Professor in the Department of Electrical Engineering, State University of New York at Stony Brook. Since 1993, he has been with the Department of Electrical and Computer Engineering, National University of Singapore, where he is currently a Professor. His current research interests are in robust control, systems theory, and the development of UAV helicopter systems.

He is a Fellow of IEEE and is the author/coauthor of seven research monographs including and *Robust and H_∞ Control* (New York: Springer, 2000); *Linear Systems Theory: A Structural Decomposition Approach* (Boston: Birkhäuser, 2004); and *Hard Disk Drive Servo Systems* (New York: Springer, 1st Ed. 2002, 2nd Ed. 2006). He was an associate editor for *IEEE Transactions on Automatic Control, Asian Journal of Control, Automatica,* and *Control & Intelligent Systems*. He is currently serving as an associate editor of *Systems & Control Letters, Journal of Control Science and Engineering,* and *Transactions of the Institute of Measurement and Control*, and an editor-at-large of *Journal of Control Theory & Applications*.

Miaobo Dong born in October 1976, received his Ph.D. degree in Control Science and Technology in 2002 from Zhejiang University, China. From 2002 to 2004, he was a postdoctoral research fellow in the State Key Laboratory of Intelligent Technology and Systems at Tsinghua University. From 2005 to 2007, he was a research fellow with the Department of Electrical and Computer Engineering, National University of Singapore. His areas of interest are the development of software systems for unmanned aerial vehicles, intelligent control, software enabled control and autonomous control.

Kai Yew Lum is principal research scientist at Temasek Laboratories of the National University of Singapore and, concurrently, teaching associate in the Department of Electrical and Computer Engineering. He received his Diplôme d'Ingénieur from the Ecole Nationale Supérieure d'Ingénieurs Electriciens de Grenoble, France in 1988, and his M.Sc. and Ph.D. from the University of Michigan, Department of Aerospace Engineering, in 1995 and 1997, respectively. He worked in the DSO National Laboratories, Singapore as junior engineer from 1990 to 1993, then as senior engineer from 1998 to 2001, specializing in control and guidance technologies. He joined the National University of Singapore in 2001. Currently, he is the principal investigator of research programmes in control, guidance and multi-agent systems. His research interests include nonlinear dynamics and control, predictive guidance, estimation and optimization. He is a member of IEEE Control Systems Society, AIAA, and the Instrumentation and Control Society of Singapore.

Tong H. Lee received the B.A. degree with First Class Honours in the Engineering Tripos from Cambridge University, England, in 1980; and the Ph.D. degree from Yale University in 1987. He is a Professor and Senior NGS Fellow in the Department of Electrical and Computer Engineering at the National University of Singapore (NUS). He was a Past Vice-President (Research) of NUS.

Dr. Lee's research interests are in the areas of adaptive systems, knowledge-based control, intelligent mechatronics and computational intelligence. He currently holds Associate Editor appointments in the IEEE Transactions in Systems, Man and Cybernetics; IEEE Transactions in Industrial Electronics; Control Engineering Practice (an IFAC journal); and the International Journal of Systems Science (Taylor and Francis, London). In addition, he is the Deputy Editor-in-Chief of IFAC Mechatronics journal.

Dr. Lee was a recipient of the Cambridge University Charles Baker Prize in Engineering, and the 2004 ASCC (Melbourne) Best Industrial Control Application Paper Prize. He has also co-authored five research monographs, and holds four patents (two of which are in the technology area of adaptive systems, and the other two are in the area of intelligent mechatronics).